THE JOURNAL OF PHYSICAL CHEMISTRY B

Article

pubs.acs.org/JPCB

Bifunctional Photoacids: Remote Protonation Affecting Chemical Reactivity

Julia Ditkovich,[†] Tzach Mukra,[†] Dina Pines,[†] Dan Huppert,[‡] and Ehud Pines*[,†]

[†]Department of Chemistry, Ben-Gurion University of the Negev, P.O.B. 653, Beer-Sheva 84105, Israel

[‡]Raymond and Beverly Sackler Faculty of Exact Sciences, School of Chemistry, Tel Aviv University, Tel Aviv 69978, Israel

ABSTRACT: Reversible protonation (deprotonation) of a side-group is a useful and convenient way to affect the reactivity of large organic and biological molecules. We use bifunctional photoacids to demonstrate how the protonation state of a basic side-group (COO^-) controls the reactivity of the main acidic group of the photoacid (OH), both in the ground and the electronic excited state of 6-carboxy derivatives of 2-naphthol.

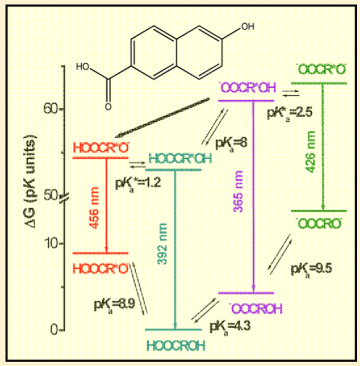

1. INTRODUCTION

Aromatic compounds substituted with a hydroxy group, like naphthols, belong to a family of very useful ROH-type photoacids, which increase their acidity typically by 5−10 pK_a units upon optical excitation.[1−4] Photoacids have been routinely used in studies of very fast (diffusion assisted) acid−base reactions. Properties of these molecules have been extensively studied and have been well characterized.[2,5−10]

Along with the increased acidity of the OH group that occurs upon electronic excitation, carboxy substituents COO^- of aromatic compounds tend to become more basic in the excited singlet state relative to their basicity in the ground electronic state. In particular, the proton donating properties of photoacids were extensively studied in recent years in conjunction with the study of the proton-accepting properties of carboxylates of simple carboxylic acids by using time-resolved IR spectroscopy.[11−19] When both the hydroxy and carboxy groups are present as two substituents on the same aromatic molecule, the mutual protonation state of the COO^- and O^- groups is expected to affect their basicity and the acidity. In *ortho*-hydroxycarboxylic acids, intramolecular proton transfer occurs via a hydrogen bond already formed in the ground state along a three-centered X-H···Y hydrogen-bonding complex, which defines the proton-transfer coordinate.

When the two functional groups are further apart, such as in the case of derivatives of 6-carboxy-2-naphthol (2N6C, Scheme 1), the proton transfer reactions of the acidic and basic groups are with the solvent, which may still couple the deprotonation and the protonation reactions of the two groups subject to the prevalence of some specific reaction coordinates similar to the ones reported for the solvent-assisted intramolecular proton transfer reactions of hydroxyquinolines.[20−23]

The paper is organized as follows: Following the Experimental and Results sections, we discuss how the acidity of the OH photoacids may be affected by the protonation state of the carboxy side-group when in the ground state. We then discuss the same effect in the electronic excited state of the photoacid where the proton transfer rates are directly accessible by time-resolved spectroscopy. Finally, we examine a unique feature of our bifunctional acids, namely, their ability to self-switch their reactivity in the excited state by transient geminate proton remote protonation of the $-COO^-$ site.

2. EXPERIMENTAL SECTION

6-Carboxy-2-naphthol (**1**) and 6-methyl-ester-2-naphthol (**2**) were purchased from TCI Japan and used as received.

Absorption and fluorescence measurements were carried out in water. Concentrations of 4×10^{-5} M of the photoacids were typically used for the spectral measurements. The H_2O was double distilled. All spectra were acquired at room temperature (23 ± 1 °C). Solutions were prepared immediately prior to spectral measurements. Absorption measurements were carried out with a HP 8452A diode array spectrometer. The fluorescence spectra were taken for the same solutions with a Cary Eclipse Spectrometer. Time-correlated single-photon counting (TCSPC) measurements were performed in Tel-Aviv with the use of excitation from a cavity-dumped titanium:sapphire femtosecond laser (Mira, Coherent), which

Special Issue: Photoinduced Proton Transfer in Chemistry and Biology Symposium

Received: September 9, 2014
Revised: November 2, 2014
Published: November 4, 2014

Scheme 1. 6-Carboxy-2-naphthol (1) and 6-Methyl-ester-2-naphthol Photoacid (2)

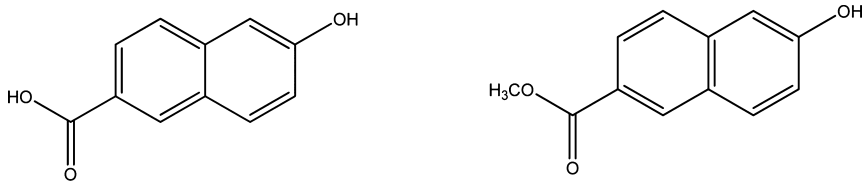

1 2

provides short, 150 fs pulses at approximately 800 nm. The second harmonic of the laser, operating over the spectral range of 380−420 nm, was used to excite the samples. The cavity dumper operated with a relatively low repetition rate of 800 kHz. The TCSPC detection system was based on a Hamamatsu 3809U photomultiplier and an Edinburgh Instruments TCC 900 computer module for TCSPC. The synthetic kinetic curves were analyzed by convolution with the instrument response function (35 ps at fwhm) and then matched with the experimental kinetic data using Matlab software version 7.2.

3. RESULTS

3.1. Steady-State Ground State Measurements. Figure 1 shows the absorption spectra of 6-carboxy-2-naphthol (2N6C) as a function of the solution pH.

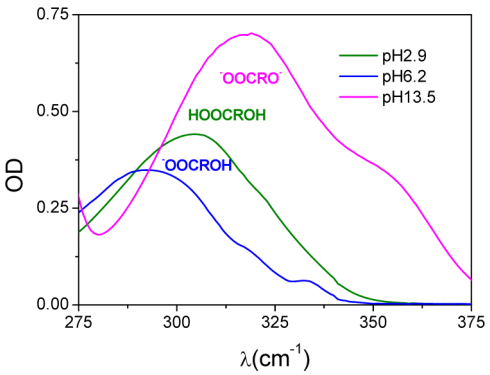

Figure 1. Absorption spectra of 2N6C in water at three representive pH values at which the monoanion (blue) the neutral (green) and dianion (violete) forms of 2N6C dominates the absorption spectra, respectively.

The absorption spectra of 6-carboxy-2-naphthol (2N6C) reveal a behavior typical of diprotic acids with two well-separated equilibrium constants. At low (very acidic) pH values, the molecule is diprotic, while in intermediate pH's it becomes amphoteric, having a weakly basic negatively charged carboxy group with a pK_a similar to that of 2-naphthoic acid (4.17) and a weakly acidic OH group with a pK_a similar to that of 2-naphthol (9.6). At high (very basic) pH's, the molecule becomes basic, and its two functional groups ionized to yield the double-charged anion, which is the conjugate base of 2N6C. The two ground-state acid−base equilibriums of 2N6C are depicted in Scheme 2.

3.2. Steady-State Excited State Measurements. The photophysics of 2N6C is much richer than the photophysics of the well-studied 2-naphthol (2N) photoacid and its derivatives, where only the ROH ↔ RO^- + H^+ equilibrium is present.

The complex behavior of the bifunctional photoacid system when in the electronic excited state is evident when considering its steady-state fluorescence spectra taken as a function of the solution pH (Figure 2).

Two isoemissive points at 386 and 448 nm appear in the fluorescence spectra and marks the existence of two acid−base equilibria in the excited state of 2N6C. In addition, a seemingly fifth fluorescent state, marked in blue in Figure 2, appears in the spectra where only four emitting states are expected to originate from the excited 2N6C system. The four emitting protonation states in the excited state are the neutral diprotic acid, HOOC−R*OH, the double ionized conjugate base of the acid, $^-$OOC−R*O^- and the two monoprotoic anions $^-$OOC−R*OH and HOOC−R*O^-. A closer inspection of the "fifth" fluorescent state shows that it is in fact a combination of the double anion fluorescence band and one of the monoanion fluorescence bands (HOOC−R*O^-). Scheme 3 summarizes the various ground and excited states of 2N6C and the proton

Scheme 2. Protonation States of 2N6C as a Function of the Solution pH[a]

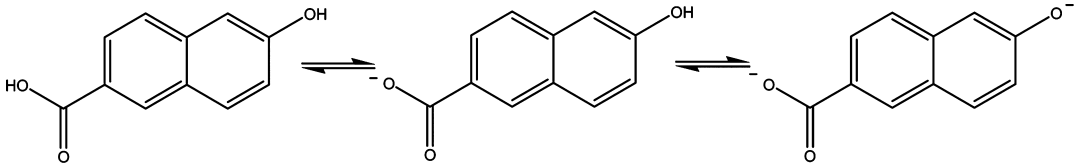

pH < 3	5 < pH < 8	pH >11
HOOC-ROH	$^-$OOC-ROH	$^-$OOC-RO^-
2N6C (neutral, diprotic)	2N6C (amphoteric)	2N6C (dianion, basic)

[a]The indicated pH range below each of the acid−base forms is the pH range at which the dominant protonation state of 2N6C is the one depicted above it.

dx.doi.org/10.1021/jp509104x | J. Phys. Chem. B 2015, 119, 2690−2701

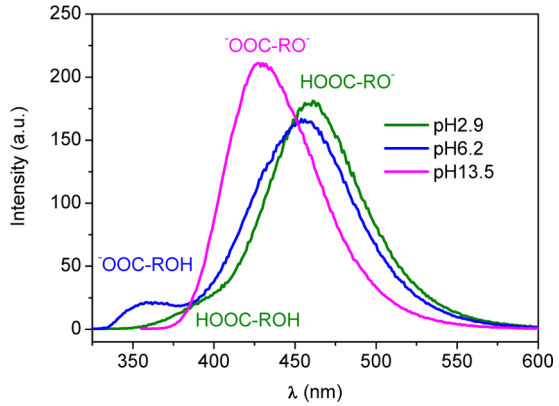

Figure 2. Steady-state fluorescence spectra of 2N6C taken at three representative pH values. The various acid–base forms of 2N6C, which are present in the excited state, and their mutual interactions are protrayed in Scheme 3 together with the coresponding ground state forms.

transfer reactions that connect between the various protonation states.

To quantitatively analyze and assign the various protonation states of the 2N6C photoacid system, we have assumed that each of the two functional groups retains its characteristic acid–base behavior as found in some reference monofunctional molecules. We have used two reference molecules for elucidating the acid–base behavior of the hydroxyl group in 2N6C: the benchmark 2-naphthol photoacid (pK_a = 9.6 and pK^*_a = 2.8)[4] and the methyl-ester derivative of 2N6C, the 2N6MC photoacid (pK_a = 8.6 and pK^*_a = 1.0), Scheme 1. In addition, 2-naphthoic acid (2NA) where only the R–COO^-↔ R–COOH equilibrium is present (pK_a = 4.17 and pK^*_a = 6.6) was used as the reference photoacid for elucidating the acid–base behavior of the carboxy group in 2N6C.

Figure 3 shows the absorption and fluorescence spectra of one of our reference molecules, the 2N6MC photoacid. A single isobathic and a single isoemissive points are clearly observed in the absorption and fluorescence spectra of 2N6MC, respectively, indicating a single well-defined acid–base equilibrium both in the ground and excited state of the molecule.

With the above reference molecules at hand, the four emitting protonation states of 2N6C have been assigned in the steady-state fluorescence spectra of the molecule. The florescence band at 456 nm was assigned to a combination of 73% of the monoanion HOOC–RO^- band at 456 nm and 27% of the dianion $^-$OOC–RO^- fluorescence band at 426 nm. The full assignment of the various protonation states of excited 2N6C and their respective emitting wavelength maxima are listed in Table 1.

With the complete band and protonation-state assignments at hand, it is feasible to carry out the Förster cycle analysis in order to estimate the pK^*_a values for each of the protonation states in the excited state of 2N6C. The relation between the observed spectral shifts and the change in the proton acidity ΔpK_a upon an electronic excitation may be written in a compact form using the difference in the 0–0 transition energies of the acid and base states expressed by the electronic transition frequencies $\Delta\nu$ (cm^{-1}), eq 1:

Scheme 3. Four Emitting Protonation States of 2N6C in the Excited State[a]

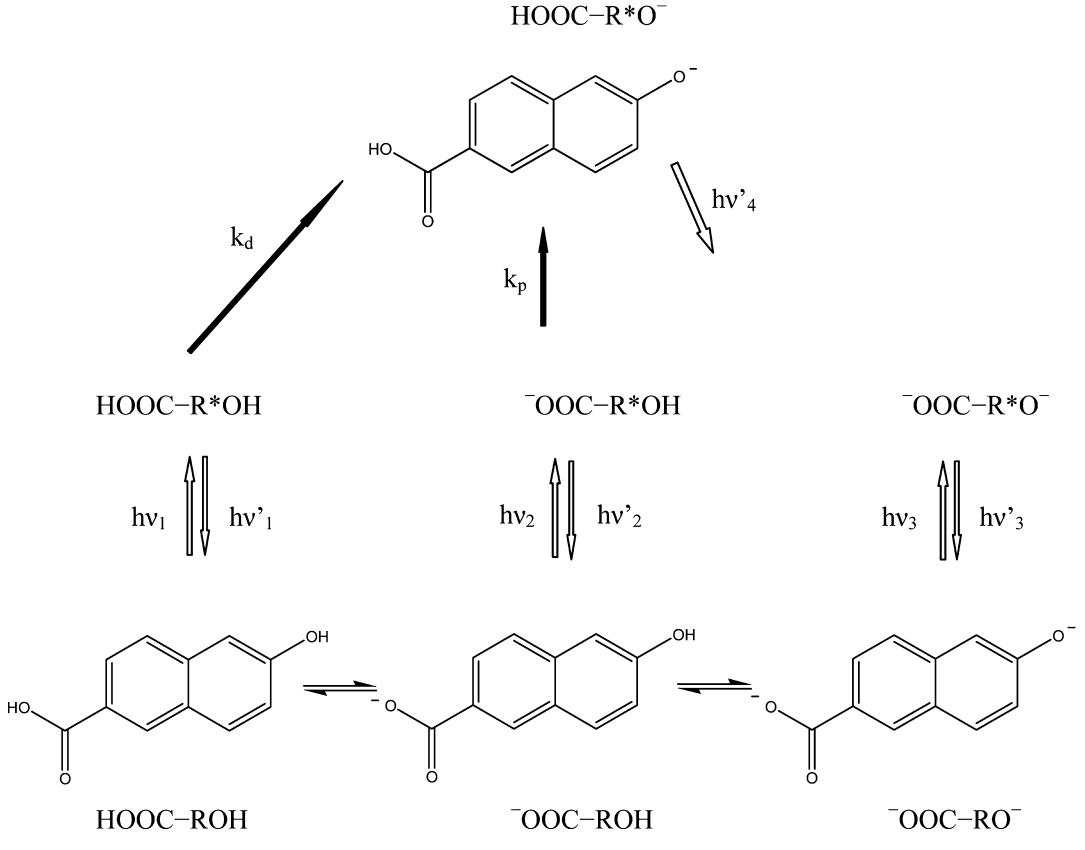

[a]Only three of the protonation states are directly accessed from the ground electronic state.

dx.doi.org/10.1021/jp509104x | J. Phys. Chem. B 2015, 119, 2690–2701

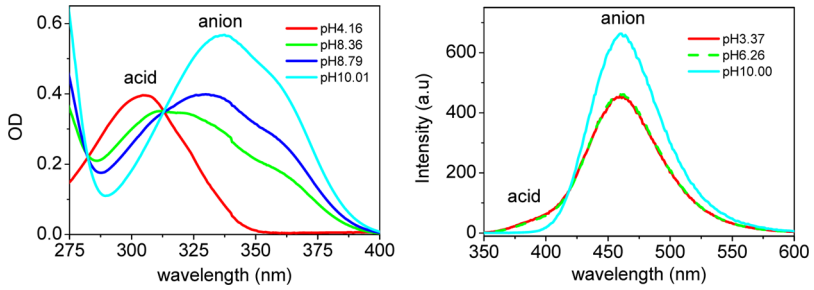

Figure 3. Absorption (left) and fluorescence spectra (right) of 2N6MC at different solution pH values.

Table 1. Spectroscopic Assignment of the Fluorescence Spectra of 2N6C

	λ_{max} Absorption [nm]	λ_{max} Fluorescence [nm]
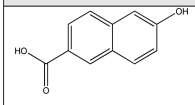 HOOC-ROH	305	392
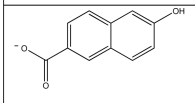 $^{-}$OOC-ROH	292	365
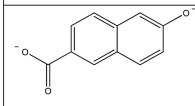 $^{-}$OOC-RO^{-}	318	426
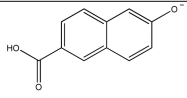 HOOC-RO^{-}	--	456

$$\Delta pK_a = pK_a^* - pK_a = (0.625\ K/T)(\Delta\nu/cm^{-1}) \quad (1)$$

The average spectral shifts in the maxima of the absorption and fluorescence spectra of the photoacid and photobase have been used in calculating $\Delta\nu$, and T is the absolute temperature in Kelvin. Table 2 summarizes the spectroscopic and thermodynamic data used in the Förster cycle calculations of the pK_a^* values of the photoacids.

3.3. Time Resolved Fluorescence Measurements. We have employed time-correlated single photon counting techniques (TCSPC) in order to monitor the time behavior of the photoacids when in their electronic excited first singlet state (Figure 4). The dynamics of 2N6C were fitted by convoluting exponential functions, which are solutions of rate equations with the instrument response function, and then best-fitting the synthetic rime-resolved reaction curves with the measured one.

We have measured the time-resolved fluorescence at pH 13.00 when both the OH moiety and the COOH side group of the photoacid were already deprotonated in the ground state (the double anionic state of 2N6C) and compared it to the time-resolved spectra of the photoacid when excited at pH = 2.89 (Figure 4a). In the latter case, the neutral molecule was excited followed by proton dissociation of the OH group to form the HOOC−R*O$^-$ anion. The deprotonation reaction is recorded in Figure 4b as the decay of the acid population and the rise-time of the monoanion product.

Table 2. pK_a^* and pK_a Values of Photoacids That Are Discussed in the Text[a]

photoacid	pK_a^0 (OH)	pK_a^* (OH)	ΔpK_a (OH)	pK_a^0 (HO_2C)	pK_a^* (HO_2C)	ΔpK_a (HO_2C)
2N6C (HOOC-ROH)	**8.9**[b]	**1.4**	**-7.5**[c]	**4.3**	**7.8**	**3.5**
2N6C ($^{-}$OOC-ROH)	**9.5**	**2.5**	**-7.0**	-	-	-
2N6M (H_3COOC-ROH)	**8.6**	**1.0**	**-7.6**	-	-	-
2N (ROH)	**9.6**	**2.8**	**-6.8**	-	-	
2NA (HOOC-R)	-	-		**4.2**	**6.6**	**2.4**

[a]When not indicated otherwise, pK^*_a values are from Förster cycle. [b]Calculated using σ_p versus pK^o_a correlation, see Discussion. [c]Shift in the maxima of the fluorescence spectra of the photoacid and photobase have been used in calculating $\Delta\nu$.

We have found (Figure 5a) that the dissociation rate of the OH photoacid depends on the protonation state of the COOH side group. At pH 2.89 we find that the acid population decay with exactly the same time constant as the rise of the fluorescence of the deprotonated product, which was 0.41 ns (Figures 4 and 5a). However, at pH 6.2, when the COOH side group was deprotonated in the ground state, the dissociation of the OH group was slowed down by a factor of 3, to 1.19 ns (Figure 5a).

A closer inspection of the time-resolved dissociation curves (Figure 5) reveals finer details of the proton dissociation curves. At pH 2.89, the dissociation lifetime is 3 times shorter than the proton dissociation at pH 6.2, but the dissociation curve exhibits a very long dissociation tail characteristic of a reversible geminate recombination of the proton as revealed by plotting the dissociation curve on a logarithmic scale (Figure 5b). The time decay of the fluorescence tail exhibits a $t^{-3/2}$ dependence over time at long times after correcting for the finite fluorescence lifetime of the band, which was 4.5 ns.[28−30] A similar $t^{-3/2}$ power law decay was observed for many OH photoacids[31−34] and was rationalized analytically by invoking a diffusion-assisted reversible geminate recombination model.[35−38]

To show that the excited state proton dissociation reaction of HOOC−R*OH is indeed reversible, the time-resolved dissociation of HOOC−R*OH was measured in acidic pH. Figure 6 shows the time-resolved dissociation of 2N6C at pH

dx.doi.org/10.1021/jp509104x | J. Phys. Chem. B 2015, 119, 2690−2701

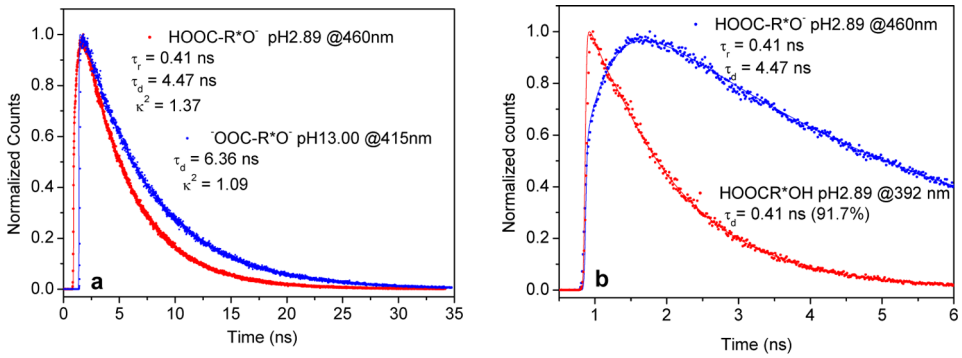

Figure 4. (a) Time correlated single photon counting decays of the $^{-}$OOC−R*O^{-} double anion, measured at 415 nm in H_2O following direct excitation at pH 13.00 (blue dots) and of HOOC−R*O^{-} the monoanion product following the dissociation of the neutral photoacid HOOC−R*OH at pH 2.89 (red dots). The decay time constants are 6.36 ns of the dianion and 4.47 ns of HOOC−R*O^{-}. (b) Time-correlated single photon counting of decay of HOOC−R*OH measured at 392 nm at pH 2.89 (red dots, the decay time constant is 0.41 ns). The complementary rise and decay curve of HOOC−R*O^{-} from panel a, shown in shorter time scale (blue dots, the rise time constant is 0.41 ns).

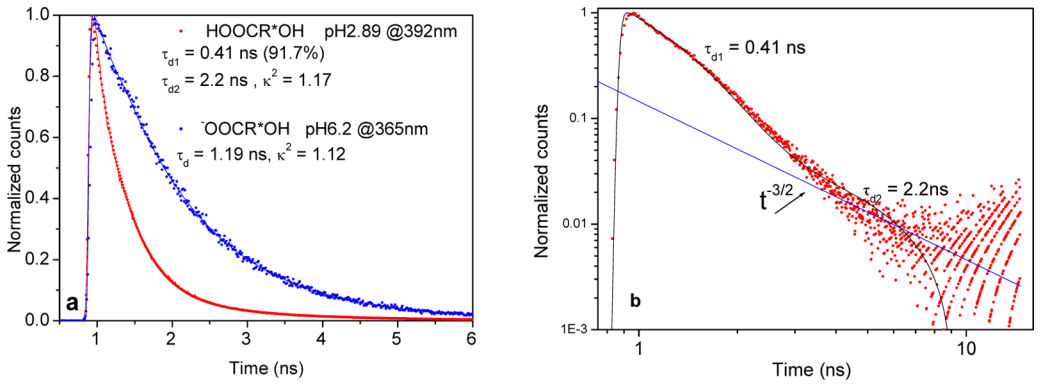

Figure 5. (a) Time-correlated single photon counting decays of HOOC−R*OH measured in H_2O at 392 nm at pH 2.89 (data from Figure 4b, red dots) and of $^{-}$OOC−R*OH (blue dots) measured at 365 nm at pH 6.2. Solid lines are the convolution exponential decays with the instrument response function. The decay time constants are 0.41 and 1.19 ns, respectively. (b) Log−log plot of the decay of the HOOC−R*OH shown in panel a after the data was multiplied by $\exp(\tau_f/t)$ to correct for the finite fluorescence lifetime, which is the excited state lifetime of the HOOC−R*O^{-} monoanion. The nonexponential long-time fluorescence tail shown in panel b is the "fingerprint" of a diffusion-assisted reversible germinal recombination process, which reforms the HOOC−R*OH form without quenching it back to the ground state.[24−27] The best biexponential fit (black curve) fails to reproduce the experimental data.

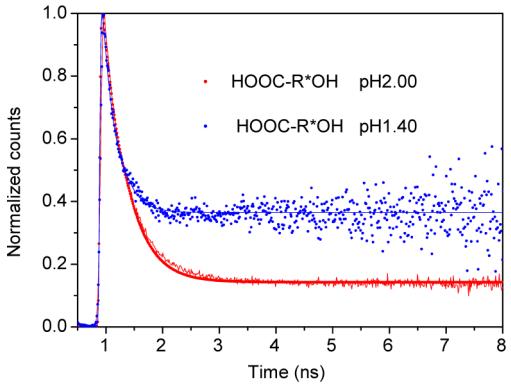

Figure 6. Time-correlated single photon counting decays of HOOC−R*OH measured at 355 nm at acidic pH's, pH = 2.00 and 1.40. The TCSPC data were multiplied by $\exp(\tau_f/t)$ to correct for the finite fluorescence lifetime, which was the excited state lifetime of the HOOC−R*O^{-} monoanion.

1.2 and 1.6. The TCSPC data were multiplied by $\exp(\tau_f/t)$ to correct for the finite fluorescence lifetime, which was the excited state lifetime of the HOOC−R*O^{-} monoanion. With increasing bulk proton concentration, the equilibrium plateau developed and became higher (Figure 6).[38−40] From this data, the value of the excited state equilibrium constant as calculated by the Förster cycle could have been verified according to

$$K_{eq} = [H^+][RO^{*-}]_{eq}/[R^*OH]_{eq} \quad (2)$$

The calculation yielded $pK^*_a = 1.2$, in good agreement with the Förster cycle value of 1.4. In the discussion of the manuscript, we use the pK_a value of 1.2 found from the excited state equilibrium instead of the pK_a value of 1.4 calculated from the Förster cycle and shown in Table 2.

The reversibility of the proton transfer reaction, which was observed in solution pHs where the carboxy group is fully protonated in the ground state (pH < 3.0), is not apparent in neutral pHs such as when the excited state proton dissociation was measured at pH 6.20 (Figure 5a). A closer inspection of the decay of the acid population and the rise of the population of its conjugate base (Figure 7) shows that the decay of the acid population and the rise of the conjugate base population are well described by a single, identical exponent (1.20 ns). Unlike the situation pertaining to pH 2.89, no indication of an appreciable reversible geminate recombination process was found, although in this case the anion was doubly charged. However, inspection of the fluorescence decay of the product

dx.doi.org/10.1021/jp509104x | J. Phys. Chem. B 2015, 119, 2690−2701

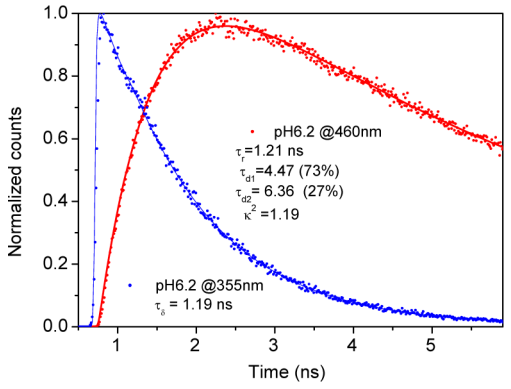

Figure 7. Time-correlated single photon counting decays of the monoanion $^-$OOC−R*OH taken at pH 6.2 and measured at 355 nm and the product of proton transfer reaction measured at 460 nm. Solid lines are the convolution exponential decays with the instrument response function. The decay of $^-$OOC−R*OH is monoexponential with time constant 1.19 ns. The signal at 460 nm rises with 1.19 ns time constant and decays with two decaying components 4.47 ns (73%) and 6.36 ns (27%).

anion revealed two decay components with about 3/4 of the anion population decaying with a lifetime of 4.50 ns, similar to the anion lifetime found at much lower pH's where the fluorescence decay is of the HOOC−R*O$^-$ monoanion. Only about 1/4 of the anion population decayed with the lifetime characterizing the decay of the proton dissociation product, $^-$OOC−R*O$^-$ (6.40 ns). All the above observations strongly imply that the proton under the above reaction conditions dominantly recombines at neutral pHs with the COO$^-$ group rather than with the O$^-$ group.

As an additional check, we have measured the fluorescence lifetime of the carboxyester derivative H_3COOC−RO$^-$ at high pH when the anionic form of the molecule was excited directly from the ground state, a situation that is not attainable for HOOC−RO$^-$ as HOOC−RO$^-$ only exists in the excited state since in the ground state the −OH group is is much less acidic than the HOOC− group (Figure 8).

We have found fluorescence lifetime that was practically identical with both the short fluorescence lifetime component found when the $^-$OOC−ROH monoanion of 2N6C was excited at pH = 6.20 and the fluorescence lifetime of the anion product of H_3COOC-ROH when it was excited at pH = 4.30 to yield H_3COOC−RO$^-$ (Figure 9).

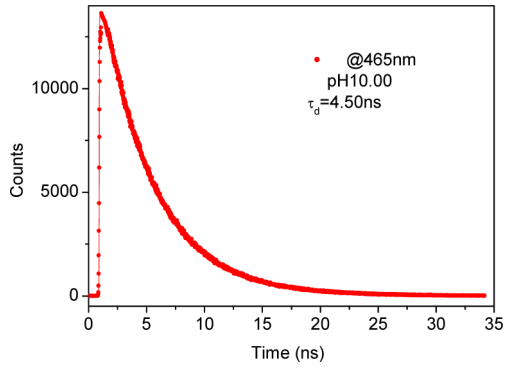

Figure 8. Time-correlated single photon counting decays of the 2N6MC anion measured at 465 nm after its direct excitation at pH 10.00 (dots). The decay time constant is 4.50 ns.

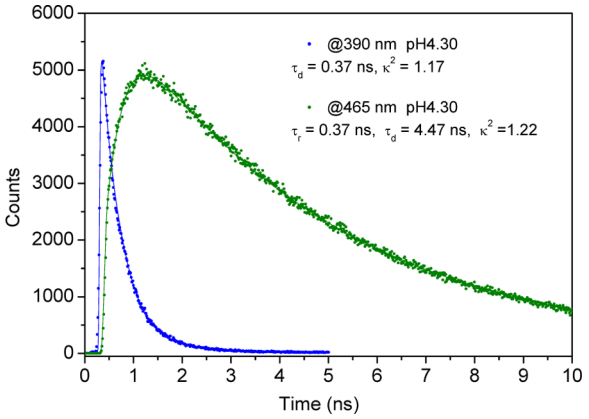

Figure 9. Time-correlated single photon counting decays of the excited acid form of 2N6MC at pH 4.30 measured at 390 nm and the product anionic form of 2N6MC measured at 465 nm. The decay of acid is monoexponential with a time constant of 0.37 ns. The anion rises within 0.37 ns and decays within 4.50 ns.

4. DISCUSSION

4.1. Remote Protonation Affecting Ground and Excited State Acidities of ROH Photoacids. The free-energy levels of the various protonation states of bifunctional photoacids may be drawn using a double Förster cycle diagram where on the left side of the diagram the side group and the main functional group (the functional group responsible for photoacidity) are both protonated in the ground state, and on the right side of the diagram only the main functional group is protonated in the ground state. In the case of 2N6C, protonation of the COO$^-$ side group increases the acidity of the ground state photoacid by 0.6 pK_a units, while in the excited state the protonation of the COO$^-$ group increases the photoacidity of the OH group by 1.3 pK_a units (Scheme 4).

Scheme 4. Free-Energy Levels of the Various Protonation States of 2N6C

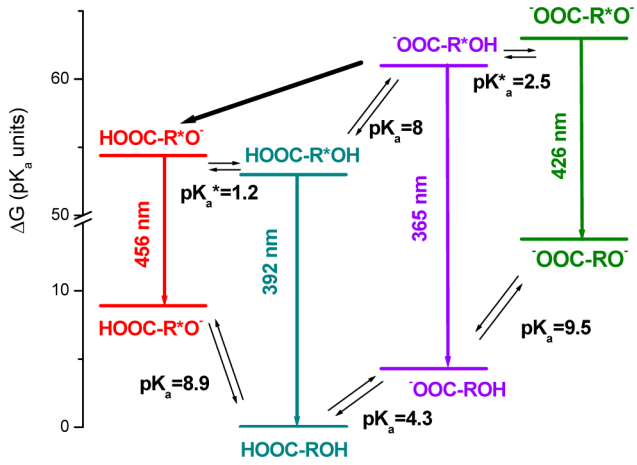

One may generalize these observations by analyzing the effect of various substituents on the ground and excited state acidity of 2-naphthol. The substituent effect on the acidity of aromatic molecules has been traditionally quantified by the Hammett σ value of the substituent. In accordance with the structure of our photoacid of interest, 2N6C, we have analyzed the substituent effect of various electron withdrawing and

dx.doi.org/10.1021/jp509104x | J. Phys. Chem. B 2015, 119, 2690−2701

donating groups at the 6 position (C-6) of the 2-naphthol aromatic ring system by using our data as well as literature data.

In Figure 10, the Hammett σ values of the various substituents are plotted against the equilibrium constant values

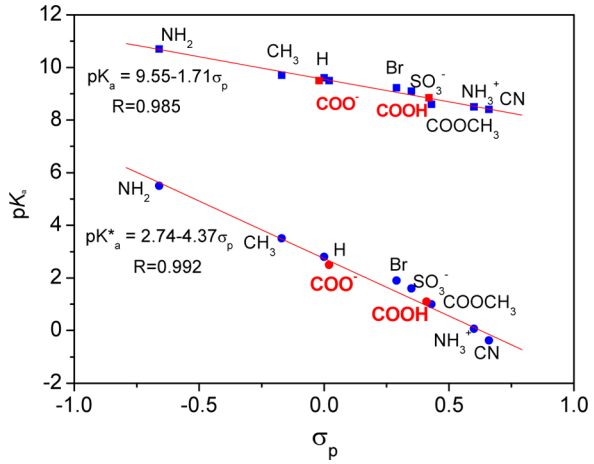

Figure 10. pK_a^0 and pK_a^*[2−5,34,44−47] values versus Hammett's σ_p[43,48] values for 2-naphthol substituents at the C-6 position. The ρ and R values of the correlations are indicated in the figure. (The pK_a value of HOOC−RO$^-$ was found by using the above correlation.)

of the corresponding photoacids in the ground and the excited state. Evidently, ring-substituents at the 6-position of the 2-naphthol ring affect K_a and K_a^* in a similar way, with K_a^* having a greater sensitivity to the substituent effect. In ref 19, we have concluded that one may discuss the effect of various types of substituents on the photoacidity of 1-naphthol derivatives using arguments and terminology that have been traditionally used for ground state acids. This conclusion was drawn from the analysis of the substituent effect mainly at the 5-C position of 1-naphthol and also at some other ring positions. In particular, using the vast body of work of Hammett[41] and Taft,[42,43] one may conclude that structure−reactivity arguments are also valid for the excited state of aromatic acids but with scaling factors different than in the ground state, i.e., aromatic acids exhibit in the electronic excited state different ρ values in the Hammett Equation than their corresponding ρ values when in the ground state.[7] For the 2-naphthol family of the 6-C substituents we have found a ρ value for the excited state equilibrium constant about 2.5 times larger than the ρ value found in the ground electronic state of the same set of photoacids (Figure 10). Similarly, for the 1-naphthol family of the 5-C substituents, we have found a ρ value for the equilibrium constant about twice larger in the excited state than in the ground electronic state of the same set of photoacids.[19]

One may quantitatively discuss the effect of remote protonation on the acidity of the main functional group of OH photoacids by considering three of the most abundant protonatable side groups: OH/O$^-$, COOH/COO$^-$, and NH_3^+/NH_2 (Table 3). Each of the six possible functional groups belonging to the three acid/base pairs may undergo a reversible protonation/deprotonation process, which will cause a significant change in the acidity of the main functional group of a bifunctional photoacid. One may estimate the pK_a change of a photoacidic group caused by remote protonation (deprotonation) according to

Table 3. List of σ_p Values of Protonatable Side Groups of Aromatic Acids

substituent	σ_p[43,48] (benzoic acid)
H	0.0
O$^-$	−0.81
OH	−0.37
CO_2^-	0.02
COOH	0.41
NH_2	−0.66
NH_3^+	0.6

$$\Delta pK_a = [\sigma_p(\text{acid form}) - \sigma_p(\text{basic form})]\rho \quad (3)$$

For the 2N6NH_3^+/2N6NH_2 pair, σ_p (acid form) − σ_p (basic form) = 1.22, and ρ for the 2N6X system, where X denotes the substituent susceptible for remote protonation, was found to be 1.71 in the ground state. By eq 3 we then get $\Delta pK_a = 1.22 \times 1.71 = 2.09$, which is in excellent agreement with the experimental value, pK_a (2N6NH_3^+) = 8.5, pK_a (2N6NH_2) = 10.7, and ΔpK_a = 2.2. In the excited state, the change in the photoacidity of the photoacid is projected to be about 2.5 larger, $\Delta pK^*_a = 1.22 \times 4.37 = 5.42$! These are very considerable acidity changes caused by a single protonatable site, which is remotely located away from the main acidic group of the molecule.

With a carboxylic side-group acting as the remote protonation site, the acidity changes are more modest but still significant, σ_p (acid form) − σ_p (basic form) = 0. 39 (based on our literature survey, there is about 10% uncertainty in this value), which experimentally translates to a pK_a change of 0.6 units and a pK^*_a change of 1.3 units with an average error bar of ±0.1 pK_a (pK^*_a) units (Scheme 3).

4.2. Remote Protonation Affecting Proton Transfer Rates as Demonstrated by Time-Resolved Measurements of 2N6C. Structure−reactivity or free-energy correlations connect between proton-transfer rates and the acidity strength (pK_a or pK^*_a) of acids and photoacids. This was first observed by Brønsted who formulated for that end the Brønsted correlation.[49]

Several modern-day analytic treatments describe this correlation quantitatively. We have shown in several publications that the Marcus correlation[50−52] and the Marcus Bond-Energy-Bond-Order (BEBO) expression[53] give good semiempiric correlations between proton equilibria and proton transfer rates. Excluding the discussion of an Inverted Region for proton transfer, which is unlikely to be observed for regular proton transfer reactions that take place along hydrogen-bonds, one can distinguish between two regions in the free-energy correlation. In the deeply endothermic region of proton transfer, the correlation is linear with a constant slope (the Brønsted coefficient), while in the exothermic part of the correlation, the slope gradually becomes smaller, signaling that in this reaction region the proton transfer rate is less sensitive to changes in the pK_a or pK^*_a of the acid.

Here, we briefly discuss one of the most successful free-energy models for proton transfer, the Marcus BEBO model.[53] The Marcus BEBO model accounts semiempirically for the observed free-energy correlations found in many proton transfer reactions in general and in photoacid proton dissociations in particular. In Figure 11, we have plotted the available thermodynamic and kinetic data for several 6-substituted 2-naphthol derivatives and several 1-naphthol and

dx.doi.org/10.1021/jp509104x | J. Phys. Chem. B 2015, 119, 2690−2701

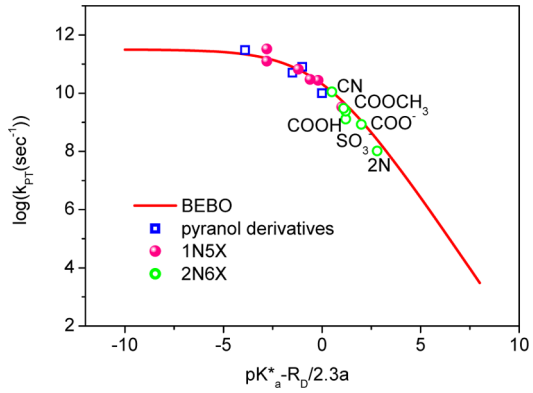

Figure 11. Free-energy correlation found in the proton dissociation reaction of 2-naphthol derivatives (2N6X). Also shown in the correlation are the kinetic rate constants for the pyranol derivatives[59] and 1-naphthol derivatives (1N5X).[19] All reaction rates were taken at room temperature. The solid line is the Marcus BEBO equation, eq 4. The parameters of the fits are log (k_o) = 11.5 for the activationless proton transfer rate and, $\Delta G^{\#}_o$ = 1.6 kcal for the intrinsic barrier common for all the proton transfer reactions. These parameters are expected to be sensitive to the exact type and the family of proton transfer reactions.

pyranol derivatives together with Marcus' BEBO correlation. Marcus and subsequently Marcus and Cohen[53] modified the electron transfer theory (ET theory) suitable for two very weakly interacting potential wells of a reactive system and applied it in a semiempiric way to proton transfer reactions by using a BEBO model for the proton-transfer coordinate along a pre-existing hydrogen-bond. In the BEBO model, bond rupture and bond formation is the principal contributor to the reaction coordinate.[53] In this case, the potential energy along the reaction coordinate is initially constant and then rises to a maximum at the transition state, after which it falls to another constant value. The activation energy is given by

$$\Delta G^{\#} = \frac{\Delta G^{\circ}}{2} + \Delta G_0^{\#} + \frac{\Delta G_0^{\#}}{\ln 2} \ln\left(\cosh\left(\frac{\Delta G^{\circ} \ln 2}{2\Delta G_0^{\#}}\right)\right) \quad (4)$$

When the driving force of the reaction ΔG^0 becomes very large, the reaction rate assumes a constant (maximal) value. It is clear that on a phenomenologic level, the BEBO model reproduces the observed free-energy correlation between rate and equilibria in many proton transfer reactions including excited state photoacid dissociations (Figure 11).

In the Kiefer and Hynes seminal papers,[54−58] Kiefer and Hynes showed that the reaction path of the proton-transfer characterized by the values of the quantum-averaged proton coordinate is very similar to the BEBO pathway and by doing so have justified the use of the readily applied Marcus' BEBO model as one of the most important semiempiric tools for correlating the reactivity of families of structurally related acids.[54,55] We conclude that Marcus' BEBO model is suitable for describing proton transfer reactions of both ground and excited state acids.

When only proton dissociation rates to water are considered, one can show by a "back of the envelope" argument that in the endothermic part of the correlation there should be a 1:1 correlation between the equilibrium acidity of an acid and its proton transfer rate to water.

The arguments goes as follows: For a general dissociation reaction of the type HX ↔ H^+ + X^-, $K_a = k_{off}/k_{on}$, where k_{off} is the overall dissociation rate constant and k_{on} is the overall recombination rate constant. For weak acids when proton dissociation is relatively slow, and the overall dissociation reaction is endothermic, the opposite recombination reaction is energetically favorable, and rate approaches the diffusion limit. For given reaction conditions, the diffusion-limited rate constant is invariable so one can write $K_a = k_{off}/k_D = k_{off}/$ constant so for this reaction region $k_{off} = cK_a$ where c is a constant formally equal to the diffusion limited recombination constant of the proton k_D.

In this region, which is applicable to most ground state acids of moderate to weak acidities, remote protonation will have a 1:1 effect on the proton transfer rate from the photoacid to water. Taking for an example the effect of the protonation state of the NH_3^+/NH_2 side-group couple on the ground state acidity constant of 2-naphthol, we have found ΔpK_a = 2.2 pK_a as the result of switching between the two protonation states of this side-group. This should translate to a $10^{2.2}$ = 160 times increase in the proton dissociation rate of 2-naphthol-6-NH_2 upon protonation of the NH_2 side group, as in Figure 11 the ground state pK_a of 2-naphthol is deeply in the endothermic region of the BEBO free-energy correlation, pK_a (2-naphthol) = 9.6.

Excited state proton transfer reactions usually belong to the second region of the free-energy correlation where change in the photoacidity cause less than a 1:1 change in the proton dissociation rate of the photoacid. Using Figure 11 as a reference, this region starts at about pK^*_a = 2.5, where the linear correlation starts to curve until reaching a plateau at very exothermic conditions. Proton transfer from electronically excited 2N6C undoubtedly belongs to the region where the free-energy correlation is curved. There, the ground state protonation of the carboxylate group caused only a 3-fold increase in the proton dissociation rate constant although the pK^*_a change was about 1.3 pK^*_a units, which for a 1:1 correlation should have been translated into 20-fold change in the excited state proton dissociation rate.

In the ground state, remote protonation has a much smaller effect on the acidity of the acid but is expected to cause a comparable change in ground state proton dissociation rate. Thus, the 0.6 pK_a increase observed upon the protonation of the carboxylate group in 2N6COO^- is expected to increase the proton dissociation rate in the ground state by $10^{0.6}$ = 4 fold.

Interestingly, as a result of the curvature in the free-energy correlation between the proton transfer rate and equilibrium constant for strong acids, the increase in the proton transfer rate upon the protonation of the side group is expected to be of a similar magnitude for the ground and excited states of 2N6C, although the projected effect on pK^*_a should be much larger than the corresponding effect on pK_a.

4.3. Remote-Protonation of the COO^- Group by Geminate Proton Recombination. Self-protonation of the naphthalene ring following excited state proton dissociation was demonstrated and kinetically analyzed for 1-naphthol.[60−62] In this case, two competing proton recombination reactions were observed. The first one, a reversible proton recombination to the oxygen atom,[24−27] and the second, irreversible proton binding to the aromatic ring, which results in quenching the molecule back to the ground state.[60−64] Pines et al.[62] developed a kinetic model, which, by means of steady-state measurement combined with simple kinetic arguments, allowed a full kinetic analysis of the two coupled geminate-recombination reaction.

dx.doi.org/10.1021/jp509104x | J. Phys. Chem. B 2015, 119, 2690−2701

A similar situation prevails in the excited state proton dissociation of 2N6C (−OOC−R*OH). There, the proton may reversibly back-recombine to the O^- group or irreversibly recombine with the COO^- side group, which is a strong base in the excited state (Scheme 5). Unlike the 1-naphthol case, the

Scheme 5. Schematic Representation of the Kinetic System of $^-$OOC−R*OH, Which Undergoes in the Excited State Two Competing Reversible Geminate-Recombination Reactions Designated by k_r and k_p

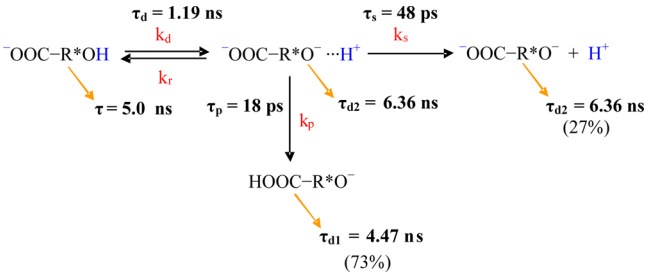

irreversible protonation of the side group does not quench the molecule but transfer the molecule to a different protonation state in the excited-state. Here we follow the kinetic treatment of Pines et al.[62] for the 1-naphthol/naphtholate system and apply it for elucidating the kinetic details of the proton geminate recombination reaction to the carboxy side group. As with 1-naphthol, the reaction is initiated in the excited state by the reversible proton dissociation of the OH group of the photoacid (2N6C).

Three steady-state rate constants are needed to characterize the reactive system of the proton-anion pair: k_s is the rate constant for the proton escaping recombination by diffusing away from the anion, k_r is the rate constant for the proton geminate recombination back to the O^- group and k_p is the rate constant for the proton geminate recombination to the COO^- side-group.

The ultimate probability for the proton to geminately recombine with the COO^- side-group, ϕ_p, is given by

$$\phi_p = \frac{k_p}{k_s + k_p} \tag{5}$$

The ultimate escape probability of the ion pair to form the free dianion and H^+ ions, is given by

$$\phi_s = 1 - \phi_p = \frac{k_s}{k_s + k_p} \tag{6}$$

rearranging we get

$$\frac{k_s}{k_p} = \frac{\phi_s}{\phi_p}; \quad k_p = \frac{\phi_p}{\phi_s} k_s \tag{7}$$

where k_s, the diffusion controlled rate constant that separates the ion pair, is given by

$$k_S = \frac{3DR_D}{r_0^3}\left[\exp\left(\frac{R_D}{r_0}\right) - 1\right]^{-1} \tag{8}$$

where D is the mutual diffusion coefficient between the ion pair, a is their contact radius, and R_D is the Debye length, which scales the coulomb interaction

$$R_D = \frac{|Z_1 Z_2| e^2}{\epsilon k_B T} \tag{9}$$

Here, Z_1 and Z_2 are the charge numbers of the two ions, e is the electron charge, ϵ is the static dielectric constant of the solvent, and k_BT is the Boltzmann factor. For the 2-naphtholate-6-COO^-−H^+ pair, we have a = 5.5 Å, $D = 10^{-4}$ cm^2 s^{-1}, and $R_D = 14.2 \times 10^{-8}$ cm in water at 298 K. We estimate the uncertainty in a and D to be less than 10% and 5%, respectively; this makes the total uncertainty in k_s less than 15%.

Substituting these parameters gives $k_s = 2.1 \times 10^{10}$ s^{-1}, which solving for k_p using eq 7 results in $k_p = 7.9 \times 10^{10}$ s^{-1}.

The complete kinetic scheme of 2N6C following electronic excitation is outlined in Scheme 5.

4.4. Verification of Remote Protonation by Geminate Proton Recombination by the Kinetic Effect of a Proton Scavenger. A useful way for verifying the existence of a diffusion-limited geminate recombination reaction of a proton is by using proton scavengers.[65] A proton scavenger is a base that recombines irreversibly to the proton when it diffuses away from its geminate anion, and by doing so terminates the geminate back recombination reaction of the proton.

Figure 12 shows steady state fluorescence measurements of 2N6C in aqueous solutions containing various concentrations of potassium formate at pH 6.2.

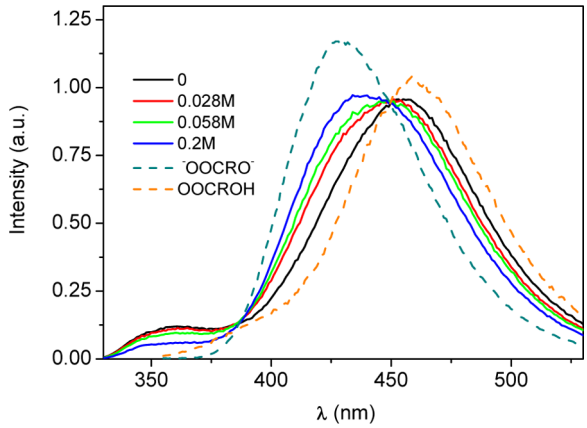

Figure 12. Steady-state fluorescence emission spectra following the optical excitation of $^-$OOC−ROH when excited at pH 6.2. The concentration of potassium formate anion was 0, 0.028, 0.058, and 0.2 M.

The quantum yield ϕ_s of the dianion $^-$OOC−RO^- increases, and the quantum yield of the monoanion ϕ_p HOOC−RO^- decreases as a function of the formate concentration (Table 4).

Table 4. Quantum Yield ϕ^{sc}_s of the Dianion $^-$OOC−RO^- in the Presence of a Scavenger Calculated from the Steady-State Fluorescence Spectra Shown in Figure 12 as a Function of the Formate Concentration

c (M)	ϕ^{sc}_s
0	27%
0.028	42%
0.056	51%
0.2	65%

dx.doi.org/10.1021/jp509104x | J. Phys. Chem. B 2015, 119, 2690−2701

The fluorescence band originating from the protonated neutral form of the photoacid excited at pH 2.80 and the fluorescence band originating from the dianion of the photoacid when directly excited at pH 13.0 are also shown for comparison.

We attribute the observed effect on the steady-state fluorescence spectra to the proton scavenging reaction by the formate anion $HCOO^- + H^+ \rightarrow HCOOH$, which is diffusion-controlled, $k_{sc} = 5 \times 10^{10}$ M^{-1} s^{-1}.

We further assume that k_{sc} depends on the ionic strength according to the Brønsted kinetic salt effect with numerical values suggested by Weller:[2]

$$\log k_{sc}(I) = \log k_{sc}(0) - \frac{1.02I^{1/2}}{1 + 2I^{1/2}} \quad (9)$$

where I is the ionic strength of the solution, which for 1:1 electrolytes is equal to the electrolyte concentration.

Following ref 60, one may define the effective lifetime of the ion-pair τ_{sc} in the presence of a scavenger as $\tau_{sc} = 1/k_{sc}(I)c$, where c is the homogeneous concentration of the scavenger. We then have, using this definition

$$\frac{\phi_s^{sc}}{\phi_s} = 1 + \frac{K\pi^{1/2}\tau_{sc}^{-1/2}}{\phi_s} \quad (10)$$

Equation 10 corresponds to the solid line shown in Figure 13.

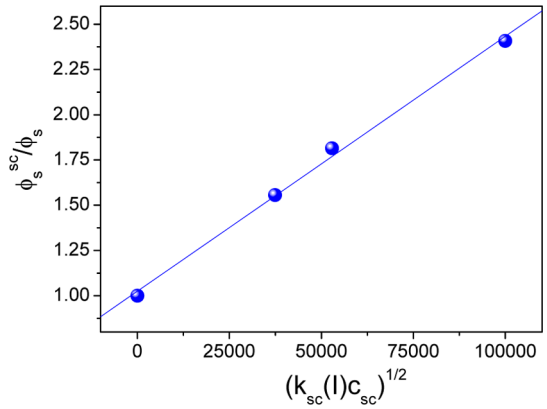

Figure 13. (ϕ_s^{sc}/ϕ_s) versus $(k_{sc}(I)c_{sc})^{1/2}$ for the proton scavenging reaction of the formate anion following the proton-dissociation of the electronically excited $^-$OOC−R*OH photoacid anion taken at pH = 6.2.

The slope of the line in Figure 13 is 1.4×10^{-5} from which one can find K, $K = 2.1 \times 10^{-6}$ $s^{1/2}$.

K is given by eq 11

$$K = \frac{\phi_s^2 a^2 k_p}{D(\pi D)^{1/2}} \exp\left(\frac{R_D}{a}\right) \quad (11)$$

Substituting for the quantum yield of the $\phi_s = 0.27$, we find $k_p = 0.13$ A/ps, which may be converted to the more common units of a first-order reaction rate using the following relation:

$$k_p(s^{-1}) = \frac{4\pi a^2 k_p}{v(a)} 10^{12}\ s^{-1} = \frac{3k_p}{a} 10^{12} \quad (12)$$

where $v(a)$ is the reaction volume having a radius of a (Å).

After the final substitution, we get $k_p = 7.1 \times 10^{10}$ s^{-1} in excellent agreement with the previous kinetic calculation, which yielded $k_p = 7.9 \times 10^{10}$ s^{-1}. We conclude that bifunctional photoacids may switch their acidity geminately, while in the excited state on a picosecond time scale by remote self-protonation. The switching of reactivity occurs by the proton dissociating from the main photoacidic group and then recombining geminately with the basic side group by bulk diffusion through the water solvent.

5. SUMMARY

We have demonstrated the effect of remote protonation/deprotonation of a side group of a large aromatic molecule on the acidity of the main reactive group of the acid. The effect is considerable both in the ground and the excited state of OH photoacids such as the 2-naphthol 6-carboxylic photoacid (2N6C) but is larger in the excited state. We find a similar significant effect of remote protonation on the proton transfer rate of the bifunctional photoacid, which we have measured directly using time-resolved fluorescence spectroscopy. We have also demonstrated that bifunctional photoacids are able to switch their reactivity on a picosecond time scale by self-remote-protonation, which occurs by the proton first diffusing through the water solvent covering the distance between the acidic group and the basic side-group and then protonating it.

Our overall kinetic modeling and our analysis of the proton geminate recombination and the remote protonation reactions as well as the modeling of the kinetic effect of the proton scavenger were all based on the proton moving through the water solvent by diffusion. Our findings negate a directed proton movement through long water wires connecting between the acid group (OH) and the basic group (COO^-). Such movement should have been on a shorter time scale and less susceptible to proton scavengers.

Finally, we find that bifunctional photoacids may be analyzed using similar ideas to the ones that were used for analyzing monofunctional photoacids with additional remote self-protonation reactions. The experimental observations described in this paper make bifunctional photoacids good candidates for further research of the effect of remote protonation and the dynamics of the through-solvent proton transfer reaction between two well-defined sites on the same molecular structure.

AUTHOR INFORMATION

Corresponding Author

*E-mail: epines@bgu.ac.il.

Notes

The authors declare no competing financial interest.

ACKNOWLEDGMENTS

This work was supported by a grant from the Israel Science Foundation 914/12 (D.H. and E.P.).

REFERENCES

(1) Förster, T. Fluoreszenzspektrum und Wasserstoffionenkonzentration. *Naturwissenschaften* **1949**, *36*, 186−187.

(2) Weller, A. Fast reactions of excited molecules. *Prog. React. Kinet.* **1961**, *1*, 187−213.

(3) Tolbert, L. M.; Haubrich, J. E. Enhanced photoacidities of cyanonaphthols. *J. Am. Chem. Soc.* **1990**, *112*, 8163.

(4) Tolbert, L. M.; Haubricht, J. E. Photoexcited Proton Transfer from Enhanced Photoacids. *J. Am. Chem. Soc.* **1994**, *116*, 10593−10600.

(5) Ireland, J. F.; Wyatt, P. A. H. Acid-base properties of electronically excited states of organic molecules. *Adv. Phys. Org. Chem.* **1976**, *12*, 131−221.
(6) Arnaut, L. G.; Formosinho, S. J. Excited state proton-transfer reactions. 1. Fundamentals and intermolecular reactions. *J. Photochem. Photobiol. A: Chem.* **1993**, *75*, 1−20.
(7) Tolbert, L. M.; Solntsev, K. M. Excited state Proton Transfer: From Constrained Systems to "Super" Photoacids to Superfast Proton Transfer. *Acc. Chem. Res.* **2002**, *35* (1), 19−27.
(8) Pines, E. UV−visible spectra and photoacidity of phenols, naphthols and pyrenols. In *Phenols*; Rappoport, Z., Ed.; PATAI's Chemistry of Functional Groups; Wiley: Chichester, U.K., 2003; Chapter 7.
(9) Nibbering, E. T. J.; Fidder, H.; Pines, E. Ultrafast chemistry: Using time-resolved vibrational spectroscopy for interrogation of structural dynamics. *Annu. Rev. Phys. Chem.* **2005**, *56*, 337−367.
(10) Pines, D.; Pines, E., Solvent assisted photoacidity. In Hydrogen-Transfer Reactions. In *Physical and Chemical Aspects I−III*; Hynes, J. T., Klinman, J. P., Limbach, H.-H., Schowen, R. L., Eds.; Wiley-VCH: Weinheim, Germany, 2007; Vol. *1*, pp 377−415.
(11) Rini, M.; Magnes, B.-Z.; Pines, E.; Nibbering, E. T. J. Real-time observation of bimodal proton transfer in acid-base pairs in water. *Science* **2003**, *301* (5631), 349−352.
(12) Rini, M.; Pines, D.; Magnes, B. Z.; Pines, E.; Nibbering, E. T. J. Bimodal proton transfer in acid-base reactions in water. *J. Chem. Phys.* **2004**, *121* (19), 9593−9610.
(13) Mohammed, O. F.; Pines, D.; Dreyer, E.; Pines, E.; Nibbering, E. T. J. Sequential Proton Transfer through Water Bridges in Acid Base Reactions. *Science* **2005**, *310*, 83−86.
(14) Mohammed, O. F.; Pines, D.; Nibbering, E. T. J.; Pines, E. Base-induced solvent switches in acid-base reactions. *Angew. Chem. - Int. Ed.* **2007**, *46* (9), 1458−1461.
(15) Mohammed, O. F.; Pines, D.; Pines, E.; Nibbering, E. T. J. Aqueous bimolecular proton transfer in acid-base neutralization. *Chem. Phys.* **2007**, *341* (1−3), 240−257.
(16) Cox, M. J.; Bakker, H. J. Parallel proton transfer pathways in aqueous acid-base reactions. *J. Chem. Phys.* **2008**, *128*, 174501.
(17) Adamczyk, K.; Prémont-Schwarz, M.; Pines, D.; Pines, E.; Nibbering, E. T. J. Real-time observation of carbonic acid formation in aqueous solution. *Science* **2009**, *326*, 1690−1694.
(18) Bakker, H. J.; Cox, M. J. Femtosecond Study of the Deuteron-Transfer Dynamics of Naphthol Salts in Water. *J. Phys. Chem. A* **2010**, *114*, 10523−10530.
(19) Prémont-Schwarz, M.; Barak, T.; Pines, D.; Nibbering, E. T. J.; Pines, E. Ultrafast Excited State Proton Transfer Reaction of 1-Naphthol-3,6-Disulfonate and Several 5-Substituted 1-Naphthol Derivatives. *J. Phys. Chem. B* **2013**, *117*, 4594−4603.
(20) Yu, H. N.; Kwon, O. H.; Jang, D. J. Migration of protons during the excited state tautomerization of aqueous 3-hydroxyquinoline. *J. Phys. Chem. A* **2004**, *108*, 5932−5937.
(21) Park, H. J.; Kwon, O. H.; Ah, C. S.; Jang, D. J. Excited state tautomerization dynamics of 7-hydroxyquinoline in *β*-cyclodextrin. *J. Phys. Chem. B* **2005**, *109* (9), 3938−3943.
(22) Kwon, O. H.; Lee, Y. S.; Yoo, B. K.; Jang, D. J. Excited state triple proton transfer of 7-hydroxyquinoline along a hydrogen-bonded alcohol chain: Vibrationally assisted proton tunneling. *Angew. Chem. Int. Ed.* **2006**, *45* (3), 415−419.
(23) Park, S. Y.; Kim, B.; Lee, Y. S.; Kwon, O. H.; Jang, D. J. Triple proton transfer of excited 7-hydroxyquinoline along a hydrogen-bonded water chain in ethers: Secondary solvent effect on the reaction rate. *Photochem. Photobiol. Sci.* **2009**, *8* (11), 1611−1617.
(24) Pines, E.; Huppert, D. Observation of geminate recombination in excited state proton transfer. *J. Chem. Phys.* **1986**, *84* (6), 3576−7.
(25) Pines, E.; Huppert, D. Geminate recombination proton-transfer reactions. *Chem. Phys. Lett.* **1986**, *126* (1), 88−91.
(26) Pines, E.; Huppert, D.; Agmon, N. Geminate Recombination in Excited State Proton-Transfer Reactions - Numerical-Solution of the Debye−Smoluchowski Equation with Backreaction and Comparison with Experimental Results. *J. Chem. Phys.* **1988**, *88* (9), 5620−5630.
(27) Agmon, N.; Pines, E.; Huppert, D. Geminate Recombination in Proton-Transfer Reactions 2. Comparison of Diffusional and Kinetic Schemes. *J. Chem. Phys.* **1988**, *88*, 5631−5638.
(28) Huppert, D.; Pines, E.; Agmon, N. Long time behavior of reversible geminate recombination reactions. *J. Opt. Soc. Am. B* **1990**, *7*, 1545−1550.
(29) Pines, D.; Pines, E. Direct observation of power-law behavior in the asymptotic relaxation to equilibrium of a reversible bimolecular reaction. *J. Chem. Phys.* **2001**, *115* (2), 951−3.
(30) Gopich, I. V.; Solntsev, K. M.; Agmon, N. Excited state reversible geminate reaction. I. Two different lifetimes. *J. Chem. Phys.* **1999**, *110* (4), 2164−2174.
(31) Masad, A.; Huppert, D. Intramolecular Proton-Transfer as a Preliminary Step for Proton Dissociation in 2-Naphthol-3,6-Disulfonate. *J. Phys. Chem.* **1992**, *96* (18), 7324−7328.
(32) Carmeli, I.; Huppert, D.; Tolbert, L. M.; Haubrich, J. E. Ultrafast excited state proton transfer from dicyano-naphthol. *Chem. Phys. Lett.* **1996**, *260*, 109−114.
(33) Leiderman, P.; Genosar, L.; Koifman, N.; Huppert, D. Effect of Pressure on the Proton-Transfer Rate from a Photoacid to a Solvent. 2. 2-Naphthol-6-sulfonate in Water. *J. Phys. Chem. A* **2004**, *108*, 2559−2566.
(34) Genosar, L.; Leiderman, P.; Koifman, N.; Huppert, D. Effect of Pressure on Proton Transfer Rate from a Photoacid to a Solvent. 3. 2-Naphthol and 2-Naphthol Monosulfonate Derivatives in Water. *J. Phys. Chem. A* **2004**, *108*, 1779−1789.
(35) Krissinel, E. B.; Agmon, N. Spherical Symmetric Diffusion Problem. *J. Comput. Chem.* **1996**, 17.
(36) Agmon, N.; Gopich, I. V. Kinetic Transition in Excited state Reversible Reactions. *Chem. Phys. Lett.* **1999**, *302*, 399−404.
(37) Agmon, N.; Gopich, I. V. Exact long-time asymptotics for reversible binding in three dimensions. *J. Chem. Phys.* **2000**, *112*, 2863−2869.
(38) Solntsev, K. M.; Huppert, D.; Agmon, N. Challenge in accurate measurement of fast reversible bimolecular reaction. *J. Phys. Chem. A* **2001**, *105*, 5868.
(39) Pines, E.; Pines, D. Direct observation of power-law behavior in the asymptotic relaxation to equilibrium of a reversible bimolecular reaction. *J. Chem. Phys.* **2001**, *115*, 951−953.
(40) Pines, E.; Pines, D., Proton dissociation and solute-solvent interactions following electronic excitation of photoacids. In *Ultrafast Hydrogen Bonding Dynamics and Proton Transfer Processes in the Condensed Phase*; Elsaesser, T., Bakker, H. J., Eds.; Kluwer Academic Publishers: Dordrecht, The Netherlands, 2003; Vol. *23*, pp 155−184.
(41) Hammett, L. P. Linear Free Energy Relationship In Rate and Equilibrium Phenomena. *Trans. Faraday Soc.* **1938**, *34*, 156−165.
(42) Taft, R. W. Polar and Steric Substituent Constants for Aliphatic and o-Benzoate Groups from Rates of Esterification and Hydrolysis of Esters. *J. Am. Chem. Soc.* **1952**, *74*, 3120−3128.
(43) Hansch, C.; Leo, A.; Taft, R. W. A Survey of Hammett Substituent Constants and Resonance and Field Parameters. *Chem. Rev. (Washington, DC, U. S.)* **1991**, *91* (2), 165−195.
(44) Rosenberg, J. L.; Brinn, I. Excited State Dissociation Rate Constants in Naphthols. *J. Phys. Chem.* **1972**, *76*, 3558.
(45) Rosenberg, J. L.; Brinn, I. M. Excited states of naphthols. Part 2.—Molecular orbital calculations on substituted naphthols1. *J. Chem. Soc., Faraday Trans.* **1976**, *72*, 448−452.
(46) Krishnan, R.; Lee, J.; Robinson, G. W. Isotope Effect on Weak Acid Dissociation. *J. Phys. Chem. A* **1990**, *94*, 6365.
(47) Huppert, D.; Tolbert, L. M.; Linares-Samanieg, S. Ultrafast Excited state Proton Transfer from Cyano-Substituted 2-Naphthols. *Phys. Chem. A* **1997**, *101*, 4602−4605.
(48) Ritchie, C. S. *Physical Organic Chemistry. The Fundamental Concepts*; Marcel Dekker: New York and Basel, 1990; p 105.
(49) Brønsted, J. N. Acid and base catalysis. *Chem. Rev. (Washington, DC, U. S.)* **1928**, *5* (3), 231−338.
(50) Marcus, R. A. Theoretical relations among rate constants barriers and Brønsted slopes of chemical reactions. *J. Phys. Chem.* **1968**, *72* (3), 891−899.

(51) Marcus, R. A. Unusual slopes of free energy plots in kinetics. *J. Am. Chem. Soc.* **1969**, *91* (26), 7224−7225.
(52) Marcus, R. A. The second R. A. Robinson memorial lecture. Electron, proton and related transfers. *Faraday Discuss.* **1982**, *74*, 7−15.
(53) Cohen, A. O.; Marcus, R. A. On slope of free energy plots in chemical kinetics. *J. Phys. Chem.* **1968**, *72* (12), 4249−4256.
(54) Kiefer, P. M.; Hynes, J. T. Nonlinear free energy relations for adiabatic proton transfer reactions in a polar environment. II. Inclusion of the hydrogen bond vibration. *J. Phys. Chem. A* **2002**, *106* (9), 1850−1861.
(55) Kiefer, P. M.; Hynes, J. T. Nonlinear free energy relations for adiabatic proton transfer reactions in a polar environment. I. Fixed proton donor−acceptor separation. *J. Phys. Chem. A* **2002**, *106* (9), 1834−1849.
(56) Kiefer, P. M.; Hynes, J. T. Adiabatic and nonadiabatic proton transfer rate constants in solution. *Solid State Ionics* **2004**, *168* (3−4), 219−224.
(57) Kiefer, P. M.; Hynes, J. T. Kinetic isotope effects for adiabatic proton transfer reactions in a polar environment. *J. Phys. Chem. A* **2003**, *107* (42), 9022−9039.
(58) Kiefer, P. M.; Hynes, J. T. Temperature-dependent solvent polarity effects on adiabatic proton transfer rate constants and kinetic isotope effects. *Isr. J. Chem.* **2004**, *44* (1−3), 171−184.
(59) Spies, C.; Shomer, S.; Finkler, B.; Pines, D.; Pines, E.; Jung, G.; Huppert, D. Solvent Fependence of Excited state Proton Transfer from Pyranine-Derived Photoacids. *Phys. Chem. Chem. Phys.* **2014**, *16*, 9104−9114.
(60) Pines, E.; Fleming, G. R. Self quenching of 1-naphthol. Connection between time-resolved and steady-state measurements. *Chem. Phys.* **1994**, *183* (2−3), 393−402.
(61) Pines, E.; Tepper, D.; Magnes, B. Z.; Pines, D.; Barak, T. Competitive geminate quenching and geminate recombination reactions of 1-naphthol. *Ber. Bunsen-Ges. Phys. Chem. Chem. Phys.* **1998**, *102* (3), 504−510.
(62) Pines, E.; Magnes, B. Z.; Barak, T. On-contact quenching of 1-naphtholate by geminate protons. *J. Phys. Chem. A* **2001**, *105* (42), 9674−9680.
(63) Agmon, N. Excited state reversible geminate reaction. II. Contact geminate quenching. *J. Chem. Phys.* **1999**, *110*, 2175−2180.
(64) Solntsev, K. M.; Agmon, N. Dual asymptotic behavior in geminate diffusion-influenced reaction. *Chem. Phys. Lett.* **2000**, *320*, 262−268.
(65) Goldberg, S. Y.; Pines, E.; Huppert, D. Proton scavenging in photoacid geminate recombination processes. *Chem. Phys. Lett.* **1992**, *192*, 77−81.